IEEE INSTRUMENTATION & MEASUREMENT SOCIETY

Received 25 November 2023; accepted 10 December 2023. Date of publication 3 January 2024; date of current version 23 January 2024.
The review of this paper was arranged by Associate Editor Amitava Chatterjee.

Digital Object Identifier 10.1109/OJIM.2023.3348904

Modeling and Analysis of Lung Water Content Using RF Sensor

PRAPTI GANGULY [1], SHREYASI DAS [2] (Student Member, IEEE), AMLAN CHAKRABARTI [1] (Senior Member, IEEE), AND JAWAD YASEEN SIDDIQUI [2] (Senior Member, IEEE)

[1]A. K. Choudhury School of Information Technology, University of Calcutta, Kolkata 700073, India

[2]Institute of Radio-Physics and Electronics, University of Calcutta, Kolkata 700073, India

CORRESPONDING AUTHOR: P. GANGULY (e-mail: pgakc_rs@caluniv.ac.in)

(Prapti Ganguly and Shreyasi Das contributed equally to this work.)

ABSTRACT Abnormal fluid buildup in the lungs, termed pulmonary edema (PE), is a result of congestive heart failure. It is a life-threatening condition, and early detection and prompt treatment can help save lives. In this article, we demonstrate the feasibility of using a microwave sensor to monitor changes in lung water content and hence detect PE. The research paper utilizes a combination of the Debye and Maxwell models, along with the Cole–Cole equation, to evaluate alterations in the dielectric properties and conductivity of lung tissue. By incorporating elements such as air and water found within the tissue, this dielectric model has been employed to foresee how lung tissues behave when subjected to different levels of hydration and inflation. A printed antenna resonating at 2.4 GHz was designed to work as a sensor. The static dielectric parameters of lung tissue at various water volume fractions were calculated at 2.4 GHz using the Debye–Maxwell model. These parameters were substituted in the Cole–Cole equation to calculate the dielectric constant of lung tissue for different levels of water in the lungs. These values were then substituted in the simulation environment, where the sensor is placed on blocks modeling the human thorax. This work is a first of its kind where the dielectric parameters at different levels of hydration have been previously estimated using mathematical models and substituted accordingly in the modeling environment to test the possibility of detection of PE with high precision. It was observed that the magnitude of the reflection coefficient values changes with increasing water volume fraction, making the microwave method of detection of PE feasible and a reliable technique.

INDEX TERMS Cole–Cole model, coupled Debye and Maxwell models, dielectric properties of lung, microwave sensor, pulmonary edema (PE).

I. INTRODUCTION

CARDIOVASCULAR diseases have always been a primary cause of hospitalization around the globe. These include chronic heart failure, acute respiratory distress syndrome (ARDS), pulmonary hypertension, kidney failure, etc. Recently, the COVID-19 pandemic created a stir and claimed about 3 million lives worldwide in a year. The fundamental step in treating these conditions is determining the patients' lung fluid volume status [1]. An abnormal build-up of fluid in the lungs is called pulmonary edema (PE). Respiratory failure occurs when there is an obstruction in gas exchange and lung mechanics caused by lung edema [2]. In critical situations, the use of mechanical ventilation is employed to sustain proper gas exchange while the edema is being treated and resolved. The current methods available for monitoring lung water, like chest X-ray and computerized tomography (CT) scan, cardiac catheterization, etc., are either expensive or invasive, making them inappropriate for continuous monitoring and early detection of PE. Hence, a device capable of measuring lung water content noninvasively with reliable accuracy is the need of the hour.

Health institutions all across the world have acknowledged the potential of wearable technology to aid medical professionals in healthcare. It is anticipated that the capabilities of wearable devices for providing health care will increase with the advancement of technology. The possible use of on-teeth sensors, smart contact lenses, electronic epidermal tattoos, smart patches, and smart textiles has been explored in a future wearables vision [3]. As a result of continuous research in the domain of wearables, more miniaturized sensors have come up, expanding the detection capabilities of sensors to include more vital signs and develop more secure and reliable data transmission networks.

Printed microwave antennas, which act as sensors, rely on the interaction of electromagnetic (EM) waves with different dielectric bodies and are designed to be extremely sensitive to changes in the permittivity of the material under consideration. Any changes in the received signal indicate variations in the permittivity due to changes in the concentration of the targeted molecules, which eventually is an alarm for potential health problems. Medical professionals have used EM wave sensing to address several medical issues, such as the amount of glucose in blood [4], to identify cancer cells [5], to determine skin moisture levels [6] and for heart monitoring [7]. The detection of pulse rate variability using an RF-based plethysmography sensor was successfully demonstrated in [8] and [9] and gave superior results compared to optical photoplethysmography sensors. The design process for wearable systems is focused on their miniaturization so that the sensors have a low profile and are lightweight and noninvasive, facilitating seamless integration of wearables into our daily lives.

The possibility of using microwave sensors to measure lung water content was first reported in [10], [11], and [12]. The work was carried forward in [13], [14], and [15], where the authors have developed a microwave sensor to measure the vital signs of the human body based on the reflection coefficient of the microwave signal transmitted through the lungs. A novel microwave sensor design developed for the purpose of measuring changes in lung water content at 2.4 GHz was reported previously by our group in [16].

Wireless communications through the human body are dependent on several factors, such as dielectric constants, conductivity and thickness of skin, properties of tissues and organs in the body, etc. These parameters are highly sensitive to frequency and, hence, must be modified to account for their great sensitivity to frequency while designing on-body sensors. The dielectric properties of biological tissues are strongly influenced by their water content [17]. This is because the polarity of the water molecules allows water to interact with an electric field. These interactions can significantly influence the tissue's overall dielectric properties [18], [19], [20]. Some prominent reasons for this are as follows.

1) *Polarization:* Water molecules can align themselves in response to an applied electric field. This process is called polarization, and it can have a substantial effect on a material's dielectric constant, which measures how much electric charge the material can store. The more water there is in a tissue, the more polarizable the tissue becomes, and the higher its dielectric constant will be [21] and [22].
2) *Ionic Conduction:* Water in biological tissues is often filled with various ions, such as sodium, potassium, and chloride. When an electric field is applied, these ions can move or conduct, resulting in an electrical current. The more water there is in the tissue, the more ions there will be, and the better the tissue will conduct electricity [22], [23].
3) *Relaxation Processes:* In the presence of an oscillating electric field, like a radio wave, polar water molecules will try to keep their alignment with the field but will always lag behind because of frictional forces. This phenomenon is called relaxation. The strength of these effects depends on the frequency of the oscillating field and the amount of water in the tissue. The more water there is, the stronger the relaxation effects and the more the tissue's dielectric properties will vary with frequency [24], [25].
4) *Interfacial Polarization:* In heterogeneous biological tissues, water often exists at interfaces between different types of cells or within cell membranes. When an electric field is applied, the charge can build up at these interfaces, resulting in a type of polarization called interfacial or Maxwell–Wagner–Sillars polarization. The amount of this polarization depends on the amount of water at these interfaces [22], [25], [26].

Therefore, as the water content in tissue changes, these effects can change as well, leading to different dielectric parameters [27]. This phenomenon is used in a variety of biomedical applications, such as dielectric spectroscopy and microwave imaging, to study tissue properties and detect diseases [28], [29], [30].

Modeling of dielectric properties of tissue has been previously reported in [27], where a comparative study of the coupled four-pole Cole–Cole and Maxwell–Fricke models and the coupled Debye and Maxwell models was presented. Debye and Maxwell models proved superior to the Maxwell–Fricke model for accurate tissue dielectric property modeling across different water content levels. It had been concluded that coupling Debye and Maxwell models required fewer assumptions and modeled tissue properties with higher accuracy, with even less than 15% mean percent error in all tissue types.

This research employs the Debye and Maxwell models in conjunction with the single-pole Cole–Cole equation to assess changes in lung tissue's dielectric properties and conductivity with superior approximation. A printed microwave antenna was used as a sensor [16] to demonstrate the possibility of capturing the change in lung water content. Leveraging tissue constituents like air and water,

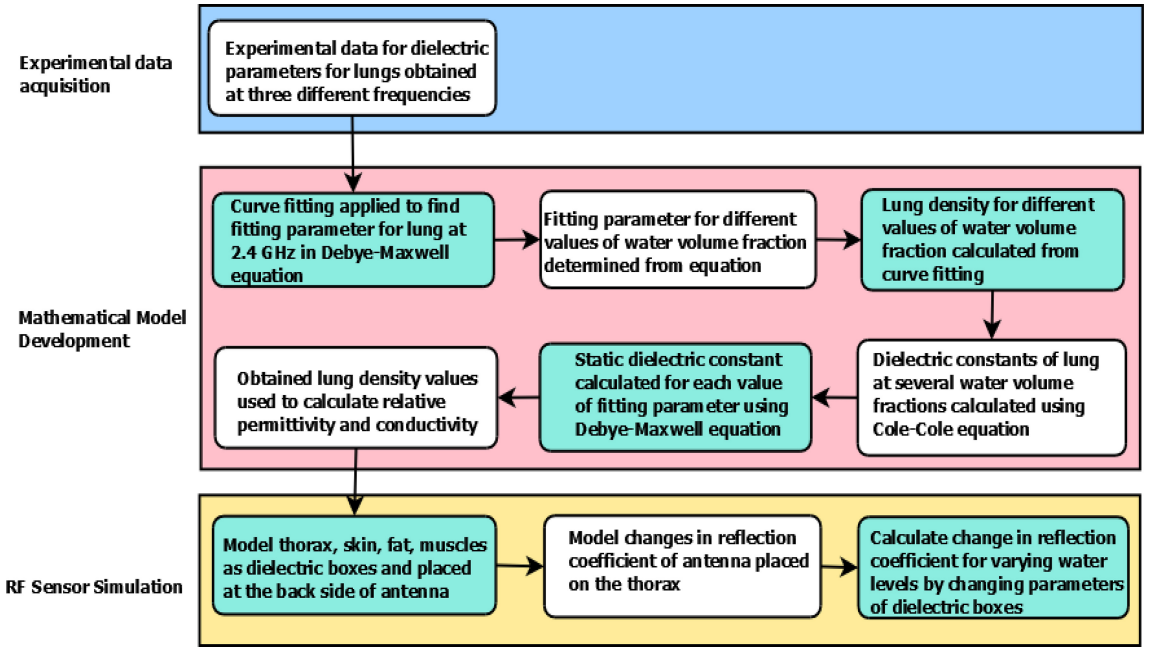

FIGURE 1. Process flow of the work.

this novel dielectric model has been utilized to predict the characteristics of lung tissues under varying hydration and inflation states, emulating conditions of PE. This model enables the construction of comprehensive tissue dielectric property models adaptable to diverse tissue types and hydration states. This is a first-of-its-kind work where the dielectric parameters of the blocks emulating human lungs have been calculated using mathematical modeling with high precision before simulating the performance of the on-body sensor. The application of these models is expected to enhance the precision of microwave ablation simulations for lung tissues. The process flow of work for this article has been summarized in the flowchart presented in Fig. 1.

II. DETERMINATION OF DIELECTRIC CONSTANT OF LUNGS

Biological tissues are often considered as lossy dielectrics. In this section, we have determined the change in the dielectric constant and conductivity of the lungs with respect to water volume fraction to emulate the condition of PE. This was accomplished by substituting the static dielectric parameters calculated using the Debye and Maxwell models in the Cole–Cole equation [31] for determining water volume fraction-dependent dielectric parameters of biological tissues. For calibration of the mathematical models, the experimental data for water volume fraction-dependent dielectric parameters of the lungs were obtained from a previously reported article by Etoz and Brace [27]. The article has reported the measured dielectric parameters of the lungs corresponding to frequencies of 1, 5.8, and 14.4 GHz. For microwave sensors placed on biological tissues, the change in the dielectric parameters of the tissues is expected to change the reflection coefficient of the antenna, which is monitored through an EM simulator [32].

TABLE I. Parameters used in (1).

Parameter	Description	Value
ε_∞	High-frequency relative permittivity	4.00
τ	Relaxation time	8.8 ps
η	Ionic conductivity	0.9 S/m
α	Distribution parameter	28×10^{-12}

The Cole–Cole model is a complex electrical impedance model used in dielectrics and bio-impedance studies to characterize the frequency-dependent behavior of polarizable materials or biological tissues [31]. It is described as the frequency f-dependent complex dielectric constant ε^* which is expressed as

$$\varepsilon^*(f) = \varepsilon_\infty + \frac{\varepsilon_s - \varepsilon_\infty}{1 + (j2\pi f\tau)^{1-\alpha}} + \frac{\sigma_i}{j2\pi f\varepsilon_0}. \tag{1}$$

The parameters in (1) are elaborated in Table I.

Since the values of the aforementioned parameters were obtained from [27] at three different frequencies, the corresponding values of the parameters at 2.4 GHz (ISM band) have been obtained by curve fitting, using [33], and the equations were further plotted using the analytical tool [34] to generate the desired graphs. In the above equation, ε_s is the static dielectric constant, which depends on the water volume fraction of the lung and is calculated using the coupled Debye and Maxwell models [27] given as

$$\varepsilon_s = \varepsilon_{sw} \times \frac{2\varepsilon_{sw} + \varepsilon_l - 2p(\varepsilon_{sw} - \varepsilon_l)}{2\varepsilon_{sw} + \varepsilon_l + 2p(\varepsilon_{sw} - \varepsilon_l)}. \tag{2}$$

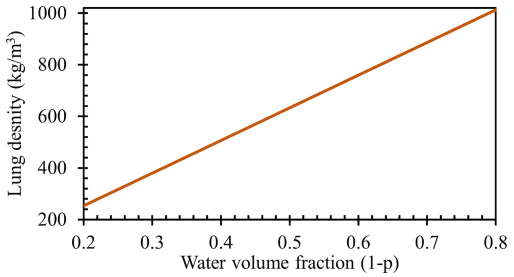

FIGURE 2. Calculated change in lung density with change in water volume percentage.

Here, ε_{sw} is the static permittivity of water, whose value is 80.0. ε_l is a fitting parameter for the lung, whose obtained value is 12.0 from the curve fitting the equation of $\varepsilon^*(f)$. The parameter p accounts for the fraction of lung water concentration and is related to the density of lung (ρ) in g/ml as

$$p = 1 - (0.79 \times \rho). \tag{3}$$

The baseline for water concentration of the lung is taken as 79% in accordance with the previously reported article [35]. The calculated values of the density of the lungs corresponding to the value of water volume fraction in the lungs have been plotted in Fig. 2. It is evident from the plot that with the increase in volume fraction of water in lungs from 20% to 80%, the lung density increases from 253 to 1013 kgm^{-3}.

The density values obtained above are used in (1) to determine the relative permittivity of the lungs, which is elaborated in Fig. 3. It is observed from the figures that the permittivity of the lung decreases with an increase in frequency. Since the biological tissues are lossy dielectrics having complex permittivity, they are expressed as

$$\varepsilon^*(f) = \varepsilon^*_{\text{real}}(f) - j * \varepsilon^*_{\text{imag}}(f). \tag{4}$$

In the above equation, the imaginary part is dependent on the conductivity of the medium and is expressed as

$$\sigma^*(f) = j2\pi f \varepsilon_0 * \varepsilon^*_{\text{imag}}(f). \tag{5}$$

Thus, the conductivity increases with an increase in the frequency as the imaginary part increases. This is further affirmed by the decrease in permittivity with frequency.

For the purpose of monitoring the change in reflection coefficient with the water volume fraction of lungs, it is desirable that the conductivity is minimized and the EM permittivity is maximized. Our desired results are obtained in the lower frequency range as demonstrated in Fig. 3.

Moreover, it is observed that for a lower range of frequencies, the change in permittivity with the water volume fraction of lungs is much greater, and the conductivity almost remains constant. Thus, the maximum change in the reflection coefficient with lung water volume fraction, which predominantly depends on the dielectric parameter of the medium, is expected to be observed at the lower frequency

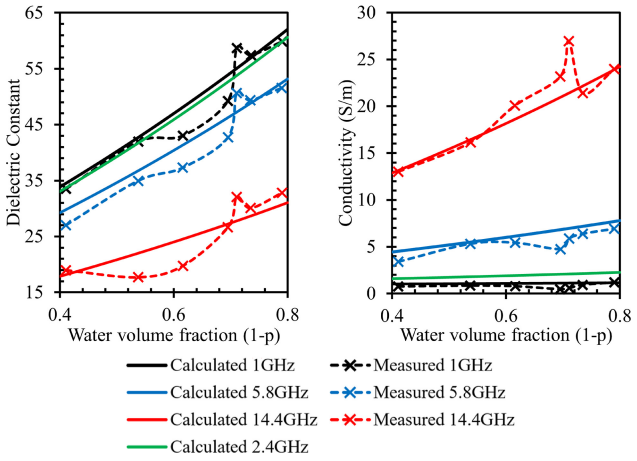

FIGURE 3. Curve-fitted lung water-dependent dielectric parameters using coupled Debye and Maxwell model parameters substituted in the Cole–Cole equation. (a) Dielectric constant. (b) Conductivity.

TABLE II. Dielectric parameters of lungs at simulated frequencies.

Volume Fraction	Permittivity	Conductivity(S/m)	Density(kg/m^3)
0.4	33.049	1.596	506.33
0.5	39.253	1.744	632.91
0.6	45.880	1.903	759.49
0.7	52.976	2.073	886.08

range. Therefore, we have selected an ISM frequency of 2.4 GHz for the purpose of our RF sensor. The obtained values of conductivities, relative permittivities, and densities corresponding to various lung water volume fractions are 2.4 GHz, which have been considered for the simulation, are listed in Table II.

III. CARDIOVASCULAR SENSOR DESIGN AND MEASUREMENT

A. SENSOR DESIGN

A novel cardiovascular sensor for monitoring cardiovascular vital signs with improved sensitivity has been demonstrated by our group previously in [16]. The antenna was a basic wave-guide applicator built on FR4 substrate(ε_r), designed to operate at 2.4 GHz, as shown in Fig. 4. Two ground structures with meandering slots encased the substrate in a sandwich arrangement.

The thickness of the FR4 substrate was taken to be 0.8 mm. The other parameters in Fig. 4 are illustrated in Table III. The structure was simulated using the EM simulator Ansys HFSS [32], and the magnitude of the reflection coefficient and 3-D far-field radiation were obtained.

B. FABRICATED RESULTS

These results for the fabricated antenna have been previously reported in [16]. It was fabricated on an FR4 substrate, as shown in Fig. 5, and the impedance parameters were measured using a vector network analyzer (VNA). The comparison of results with the simulated design is shown in Fig. 6(a). It is seen that the measured results closely follow

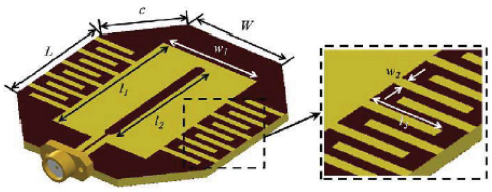

FIGURE 4. Structure of the microwave cardiovascular sensor at 2.4 GHz.

TABLE III. Dimensions of the fabricated antenna (in mm).

W	L	l1	l2	l3	w1	w2	c
20	20	27.6	23	9.5	18.4	1.05	14.14

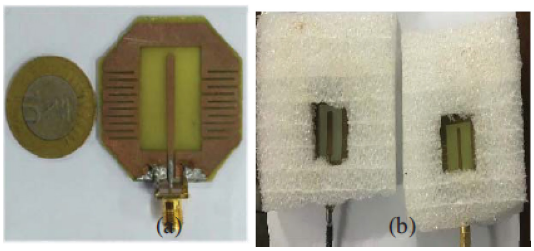

FIGURE 5. Fabricated prototype of the antenna. (a) Comparison of size of the antenna with size of a coin. (b) Experimental setup of front and back side of antenna placed inside a layer of foam.

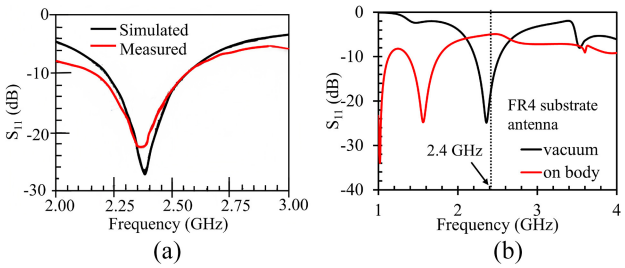

FIGURE 6. Comparison of S_{11} for antenna with FR4 substrate. (a) Simulated versus measured results in vacuum. (b) Vacuum versus on-body with 40% lung water content.

the simulated results, yielding a resonance at 2.4 GHz. When working with bio-models, it is crucial to take into account the specific absorption rate (SAR), which evaluates how much energy the human body absorbs when exposed to an RF EM field. The SAR value for our sensor was found to be 0.5 W/kg, averaged over 1 g, which was significantly less than the FCC limit of 1.6 W/kg. The gain at central frequency, i.e., 2.4 GHz for our design, was found to be 2.5 dBi, which makes it suitable for low-power applications.

However, it has also been observed that when FR4 substrate and aforementioned dimensions have been used, although desirable reflection has been obtained in a vacuum at 2.4 GHz, the antenna performance decreases significantly when placed on the body, which is observable in Fig. 6(b). Therefore, the substrate of the antenna was changed to Rogers RT Duroid 5870, which resulted in improved on-body antenna performance for the detection of lung water volume percentage changes.

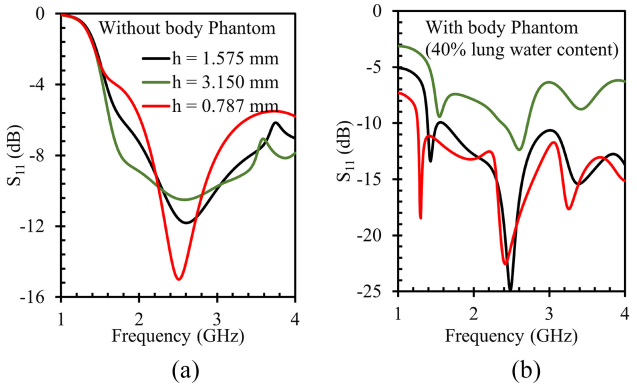

FIGURE 7. Comparison of S_{11} for the antenna with Rogers RT Duroid 5870 substrates of different thickness "h." (a) Vacuum. (b) on-body with 40% lung water.

For the antenna design reported in this work, a Rogers RT Duroid 5870 substrate of thickness 1.575 mm has been used. The reason for choosing this substrate is its much lower loss tangent of 0.0012 as compared to 0.02 of FR4 substrate. The particular substrate thickness has been selected based on its superior on-body performance. A study has been conducted for different substrate thicknesses as reported in Fig. 7(a) and (b) by monitoring the reflection coefficient (S_{11}) of the antenna with and without body phantom. It has been observed that though better antenna performance in terms of S_{11} has been observed in the vacuum for the substrate thickness of 0.787 mm, which is half of the original thickness of 1.575 mm, the S_{11} is very noisy when placed on the body phantom. As for the antenna performance with a substrate thickness of 3.15 mm, i.e., double the original thickness, the degraded antenna performance has been observed in a vacuum as well as when placed on a body phantom. No clear peak of reflection coefficient has been observed at the desired operating frequency of 2.4 GHz in this case. Therefore, the substrate thickness of 1.575 mm has been considered for further simulations.

IV. SIMULATION METHODOLOGY

In order to simulate the on-body RF sensor for measurement of lung water content, we have monitored the change in the reflection coefficient of the antenna placed on the thorax over the lung. The obtained reflection coefficient is then associated with the water volume fraction in the lung.

For the RF sensor for lung water monitoring, we have used an antenna with the Rogers RT Duroid 5870 substrate of thickness 1.575 mm. This substrate allows a broader bandwidth at the high frequency of 2.4 GHz, given its lower dielectric constant of 2.33 compared to 4.4 of FR4 substrate. Moreover, it has a lower loss tangent of 0.0012, compared to 0.02 of FR4, resulting in lower signal loss. The dimensions of the simulated antenna with

TABLE IV. Dimensions of the simulated antenna (in mm).

W	L	l1	l2	l3	w1	w2	c
20	20	25.95	21.9	8.03	23.2	0.92	14.14

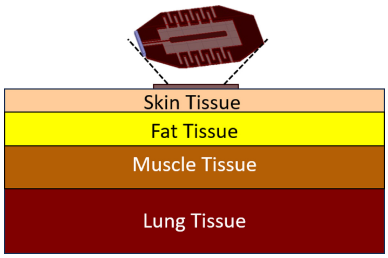

FIGURE 8. Schematic of the RF sensor placed on the thorax.

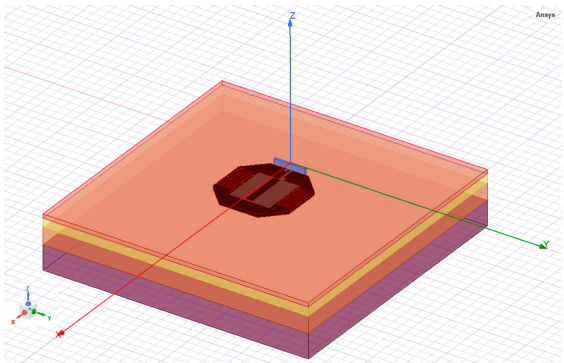

FIGURE 9. Ansys HFSS simulation schematic: RF sensor placed on the thorax region modeled as dielectric blocks.

Rogers RT Duroid 5870 substrate have been illustrated in Table IV.

A schematic view of the simulated structure is shown in Fig. 8. The layers forming the thorax region over the lung have been modeled at 2.4 GHz using lossy dielectric blocks in the Ansys HFSS environment [32], as shown in Fig. 9. This method of body phantom RF simulations has been adopted earlier in several studies [36], [37] and revealed significant coherence experimental results [15], [38]. The material parameters of the biological tissues have been obtained from [39], which are tabulated in Table V. By changing the lung parameters at different water volume fractions, obtained from the graphs in Figs. 2 and 3, we were able to replicate the accumulation of excess water in the lung, a condition called PE. The dielectric parameters, conductivity, and density of the lungs were changed in the lossy dielectric blocks to indicate the increase in water volume fraction in the lungs. The reflection coefficient of the antenna was noted at several water volume fractions, i.e., at 40%, 50%, 60%, and 70% occupancy of water in the lungs.

V. SIMULATION RESULTS

The variation in reflection coefficient (S_{11}), obtained through simulation, was plotted for different levels of water volume fraction in the lungs. The simulated results of S_{11} for different percentages of water volume are shown in Fig. 10(a).

TABLE V. Dielectric parameters of modeled dielectric blocks.

Layer	Thickness	Permittivity	Conductivity(S/m)	Density(kg/m^3)
Skin	2 mm	38	1.46	1109
Fat	4.65 mm	5.28	0.105	911
Muscle	8.67 mm	52.7	1.74	1090
Lung	12.57 mm	Calculated	Calculated	Calculated

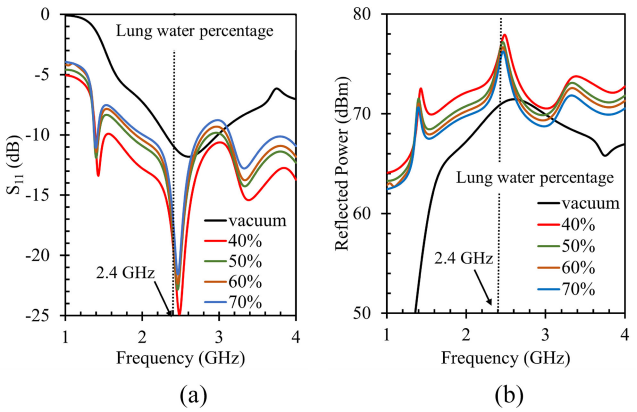

FIGURE 10. Monitored change in (a) reflection coefficient and (b) reflected power of the antenna with change in lung water volume percentage.

The minimum value of S_{11} is much lower for the antenna tested in a vacuum. However, when the antenna was placed on the blocks that imitate the human body's thorax, the return loss was relatively high at the desired frequency of 2.4 GHz, which indicates that the match between the antenna and the thorax region is good. Though the change in S_{11} when the water content increases by 10% is not very significant, a noticeable change in S_{11} is observed when the change in water level is in intervals of 20%.

The reflected power of the antenna has also been calculated from the obtained reflection coefficient. Results were obtained for the antenna placed in vacuum and on the body phantom with different lung water volume concentrations. Fig. 10(b) shows the change in reflected power at different concentrations of water in the lungs. The reflected power has been observed to decrease with an increase in the percentage of water. The radiation pattern of the antenna when placed in the vacuum has been plotted in Fig. 11(a), and that when the antenna is placed on the body phantom is plotted in Fig. 11(b). Attenuation of the signal on the back side of the antenna has been observed on placed on the body phantom due to penetration of the waves in the body, which acts like a dielectric with a very high dielectric constant.

The fat content in a human being is not constant and changes from person to person [44], [45]. In order to investigate the effect of the thickness of the fat layer on the return loss of the antenna, the S_{11} was simulated for several values of the fat layer by increasing the thickness of the fat layer model. The simulated results of the change in S_{11} with fat layer thickness are shown in Fig. 12. It is seen that the fat layer thickness does not have a significant effect on the return loss (S_{11}).

TABLE VI. Summary of existing works.

Authors	Antenna used	Freq. range	Size	Purpose	Technique	Metrics and Performance
[40]	Balanced antipodal Vivaldi antenna	1.5-6.5 GHz	80x 44x 9.2mm	Lung water monitoring	Monostatic ultra wideband radar measurements	Metric: Normalized autocorrelation, 5.6% relative error
[41]	A pair of 5x5 rectangular loop antenna	403 MHz	5cmx 5cm	Pulmonary Edema Detection	Wearable antennas on chest and back	Metric: S_{21}, 4.5dB change with 0.44 mass density change
[42]	37 port sensor on fabric textile	60MHz	length 89.4cm	Estimate dielectric constant to monitor edema	Wrapped around human torso	Metric: Dielectric constant , 0.57% error
[15]	50 ohm terminated coplanar waveguide	915-920 MHz	19.2x 22.2mm	Pulmonary Edema Monitoring	Chest patch	Metric:S_{11}, -28dB reflection coefficient
[43]	17 electrodes with 16 ports in-between	40 MHz port excitation	16cmx 10cm	Extract electrical properties of tissues beneath skin-fat-muscle layer	chest and upper abdominal patch	Meric: Permittivity, 9.8% error for normal lungs and 4.7% error for edema
This work	waveguide applicator	2.4 GHz	25mmx 25mm	Lung water monitoring	Chest patch	Metric: S_{11} ,12% change for 10% of water

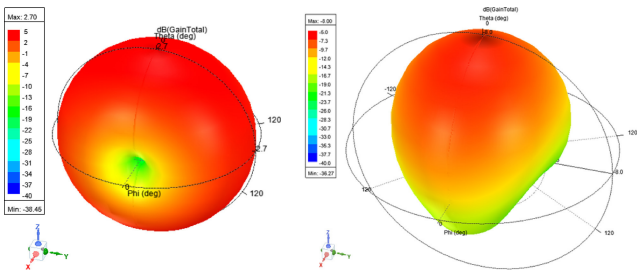

FIGURE 11. Comparison of the radiation patterns of the monopole antenna. (a) Vacuum. (b) On-body with 40% lung water.

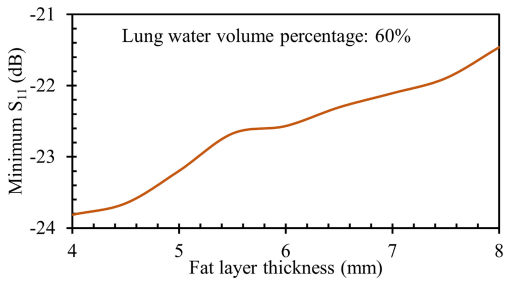

FIGURE 12. Monitored change in reflection coefficient of the lung with change thickness of the fat layer.

From the results obtained, we can claim that it is possible to detect changes in lung water content using the microwave sensor mentioned in this article. Additionally, we explore the possibility of the effect of any other parameter on the S_{11}, for example, fat thickness. However, no significant effect of the fat layer on return loss was noted. A comparison of this work with the state-of-the-art studies is presented in Table VI.

VI. CONCLUSION

The water content of biological tissues has a significant impact on their dielectric characteristics. By substituting the value of the static element of dielectric in the Debye and Maxwell models in the Cole–Cole equation, we were able to derive the dielectric constant, conductivity, and lung density at the desired frequency of 2.4 GHz. We see that the dielectric constant and the lung density change with an increase in water volume fraction in the lungs. Substituting these values in the set-up replicating the sensor placed on the human thorax, we were able to conclude that the return loss is dependent on the water volume fraction and can be used as a reliable technique to detect PE. Our future work will involve an extension of the simulated model to real-time experiments.

REFERENCES

[1] X. Cui et al., "Pulmonary edema in COVID-19 patients: Mechanisms and treatment potential," *Frontiers Pharmacol.*, vol. 12, Jun. 2021, Art. no. 664349.
[2] L. Amado-Rodríguez et al., "Mechanical ventilation in patients with cardiogenic pulmonary edema: A sub-analysis of the lung safe study," *J. Intensive Care*, vol. 10, no. 1, p. 55, 2022.
[3] R.-C. Qian and Y.-T. Long, "Wearable chemosensors: A review of recent progress," *ChemistryOpen*, vol. 7, no. 2, pp. 118–130, 2018.
[4] M. N. Hasan, S. Tamanna, P. Singh, M. D. Nadeem, and M. Rudramuni, "Cylindrical dielectric resonator antenna sensor for non-invasive glucose sensing application," in *Proc. 6th Int. Conf. Signal Process. Integr. Netw. (SPIN)*, 2019, pp. 961–964.
[5] L. Wang, "Microwave sensors for breast cancer detection," *Sensors*, vol. 18, no. 2, p. 655, 2018.
[6] R. Schiavoni et al., "Microwave wearable system for sensing skin hydration," in *Proc. IEEE Int. Instrum. Meas. Technol. Conf. (I2MTC)*, 2021, pp. 1–6.
[7] R. R. Fletcher and S. Kulkarni, "Clip-on wireless wearable microwave sensor for ambulatory cardiac monitoring," in *Proc. Annu. Int. Conf. IEEE Eng. Med. Biol.*, 2010, pp. 365–369.
[8] P. Ganguly, D. E. Senior, A. Chakrabarti, and P. V. Parimi, "Sensitive transmit receive architecture for body wearable RF plethysmography sensor," in *Proc. Asia-Pac. Microw. Conf. (APMC)*, 2016, pp. 1–4.
[9] P. Ganguly, D. E. Senior, P. V. Parimi, and A. Chakrabarti, "Wearable RF plethysmography sensor using a slot antenna," in *Proc. IEEE Int. Symp. Antennas Propag. (APSURSI)*, 2016, pp. 1169–1170.
[10] C. Susskind, "Possible use of microwaves in the management of lung disease," *Proc. IEEE*, vol. 61, no. 5, pp. 673–674, May 1973.
[11] P. C. Pedersen, C. C. Johnson, C. H. Durney, and D. G. Bragg, "An investigation of the use of microwave radiation for pulmonary diagnostics," *IEEE Trans. Biomed. Eng.*, vol. BME-23, no. 5, pp. 410–412, Sep. 1976.

[12] P. C. Pedersen, C. C. Johnson, C. H. Durney, and D. G. Bragg, "Microwave reflection and transmission measurements for pulmonary diagnosis and monitoring," *IEEE Trans. Biomed. Eng.*, vol. BME-25, no. 1, pp. 40–48, Jan. 1978.

[13] M. F. Iskander, C. H. Durney, D. J. Shoff, and D. G. Bragg, "Diagnosis of pulmonary edema by a surgically noninvasive microwave technique," *Radio Sci.*, vol. 14, no. 6S, pp. 265–269, Nov./Dec. 1979.

[14] R. Gagarin, N. Celik, H.-S. Youn, and M. F. Iskander, "Microwave stethoscope: A new method for measuring human vital signs," in *Proc. IEEE Int. Symp. Antennas Propag. (APSURSI)*, 2011, pp. 404–407.

[15] N. Celik, R. Gagarin, G. C. Huang, M. F. Iskander, and B. W. Berg, "Microwave stethoscope: Development and benchmarking of a vital signs sensor using computer-controlled phantoms and human studies," *IEEE Trans. Biomed. Eng.*, vol. 61, no. 8, pp. 2341–2349, Aug. 2014.

[16] P. Ganguly, A. Dey, D. Ganguly, C. Saha, and J. Y. Siddiqui, "WBAN channel modeling on electromagnetic interaction in biological tissues for estimating path loss characteristics," in *Proc. 14th Eur. Conf. Antennas Propag. (EuCAP)*, 2020, pp. 1–4.

[17] S. Di Meo et al., "The variability of dielectric permittivity of biological tissues with water content," *J. Electromagnet. Waves Appl.*, vol. 36, no. 1, pp. 48–68, 2022.

[18] C. Gabriel, S. Gabriel, and Y. E. Corthout, "The dielectric properties of biological tissues: I. literature survey," *Phys. Med. Biol.*, vol. 41, no. 11, p. 2231, 1996.

[19] W. Kuang and S. O. Nelson, "Low-frequency dielectric properties of biological tissues: A review with some new insights," *Am. Soc. Agr. Eng.*, vol. 41, no. 1, pp. 173–184, 1998.

[20] T. Said and V. V. Varadan, "Variation of Cole–Cole model parameters with the complex permittivity of biological tissues," in *IEEE MTT-S Int. Microw. Symp. Tech. Dig.*, 2009, pp. 1445–1448.

[21] R. Ghosh, S. Banerjee, M. Hazra, S. Roy, and B. Bagchi, "Sensitivity of polarization fluctuations to the nature of protein-water interactions: Study of biological water in four different protein-water systems," *J. Chem. Phys.*, vol. 141, no. 22, pp. 1–12, 2014.

[22] B. Legras, I. Polaert, L. Estel, and M. Thomas, "Mechanisms responsible for dielectric properties of various faujasites and linde type a zeolites in the microwave frequency range," *J. Phys. Chem. C*, vol. 115, no. 7, pp. 3090–3098, 2011.

[23] A. Aksimentiev and K. Schulten, "Imaging α-hemolysin with molecular dynamics: Ionic conductance, osmotic permeability, and the electrostatic potential map," *Biophys. J.*, vol. 88, no. 6, pp. 3745–3761, 2005.

[24] G. H. Haggis, J. B. Hasted, and T. J. Buchanan, "The dielectric properties of water in solutions," *J. Chem. Phys.*, vol. 20, no. 9, pp. 1452–1465, 1952.

[25] M. Böhning et al., "Dielectric study of molecular mobility in poly (propylene-graft-maleic anhydride)/clay nanocomposites," *Macromolecules*, vol. 38, no. 7, pp. 2764–2774, 2005.

[26] F. Zhou and K. Schulten, "Molecular dynamics study of a membrane-water interface," *J. Phys. Chem.*, vol. 99, no. 7, pp. 2194–2207, 1995.

[27] S. Etoz and C. L. Brace, "Development of water content dependent tissue dielectric property models," *IEEE J. Electrom., RF Microw. Med. Biol.*, vol. 3, no. 2, pp. 105–110, Jun. 2019.

[28] H. M. Fahmy et al., "Dielectric spectroscopy signature for cancer diagnosis: A review," *Microw. Opt. Technol. Lett.*, vol. 62, no. 12, pp. 3739–3753, 2020.

[29] L. Gun, D. Ning, and Z. Liang, "Effective permittivity of biological tissue: Comparison of theoretical model and experiment," *Math. Problems Eng.*, vol. 2017, Jun. 2017, Art. no. 7249672.

[30] H. Wang et al., "Correlation between the dielectric properties and biological activities of human ex vivo hepatic tissue," *Phys. Med. Biol.*, vol. 60, no. 6, p. 2603, 2015.

[31] K. S. Cole and R. H. Cole, "Dispersion and absorption in dielectrics i. alternating current characteristics," *J. Chem. Phys.*, vol. 9, no. 4, pp. 341–351, 1941.

[32] *Ansys HFSS Software*. (2022). Ansys HFSS. [Online]. Available: http://www.ansoft.com/products/hf/hfss/version=2022.r1.

[33] *Origin (Pro) Version 8.5*, Originlab Corp., Northampton, MA, USA, 2022.

[34] *Version 7.10.0 (R2010a)*, MathWorks Inc., Natick, MA, USA, 2016.

[35] F. A. Duck, *Physical Properties of Tissues: A Comprehensive Reference Book*. Cambridge, MA, USA: Academic press, 2013.

[36] W. Wang, X. W. Xuan, P. Pan, Y. J. Hua, H. B. Zhao, and K. Li, "A low-profile dual-band omnidirectional Alford antenna for wearable WBAN applications," *Microw. Opt. Technol. Lett.*, vol. 62, no. 5, pp. 2040–2046, 2020.

[37] S. Kiani, P. Rezaei, and M. Fakhr, "A CPW-fed wearable antenna at ISM band for biomedical and WBAN applications," *Wireless Netw.*, vol. 27, pp. 735–745, Nov. 2020.

[38] G. Gao, R. Zhang, C. Yang, H. Meng, W. Geng, and B. Hu, "Microstrip monopole antenna with a novel UC-EBG for 2.4 GHz WBAN applications," *IET Microw., Antennas Propag.*, vol. 13, no. 13, pp. 2319–2323, 2019.

[39] C. Gabriel, "Compilation of the dielectric properties of body tissues at RF and microwave frequencies," Phys. Dept., King's Coll. London, London, U.K., Rep. TR-1996-0004, 1996.

[40] J. Moll, J. Vrba, I. Merunka, O. Fiser, and V. Krozer, "Non-invasive microwave lung water monitoring: Feasibility study," in *Proc. 9th Eur. Conf. Antennas Propag. (EuCAP)*, 2015, pp. 1–4.

[41] K. Ladic, K. Sayrafian, U. Bengi, and S. Dumanli, "A wearable wireless monitoring system for the detection of pulmonary edema," in *Proc. IEEE Glob. Commun. Conf. (GLOBECOM)*, 2021, pp. 1–5.

[42] M. Tayyab, M. S. Sharawi, and A. Shamim, "A wearable RF sensor on fabric substrate for pulmonary edema monitoring," in *Proc. Sensors Netw. Smart Emerg. Technol. (SENSET)*, 2017, pp. 1–4.

[43] S. Salman, Z. Wang, E. Colebeck, A. Kiourti, E. Topsakal, and J. L. Volakis, "Pulmonary edema monitoring sensor with integrated body-area network for remote medical sensing," *IEEE Trans. Antennas Propag.*, vol. 62, no. 5, pp. 2787–2794, May 2014.

[44] A. Lemanowicz, W. Leszczyński, G. Rusak, B. Marcin, and P. Ratajczak, "Chest adipose tissue distribution in patients with morbid obesity," *Pol. J. Radiol.*, vol. 83, pp. 68–75, Feb. 2018.

[45] P. Störchle, W. Müller, M. Sengeis, S. Lackner, S. Holasek, and A. Fürhapter-Rieger, "Measurement of mean subcutaneous fat thickness: Eight standardised ultrasound sites compared to 216 randomly selected sites," *Sci. Rep.*, vol. 8, no. 1, 2018, Art. no. 16268.